Museros *et al.*
1Universitat Politècnica de València, Dpt. of Continuum Mechanics and Theory of Structures, Valencia, Spain
2KTH Royal Institute of Technology, Division of Structural Engineering and Bridges, Stockholm, Sweden
3Actividades de Infraestructuras Públicas y Conservación S.L. (AIP), Valencia, Spain
Pedro Museros, Universitat Politècnica de València, Camino de Vera s/n, 46022 Valencia, Spain.
pmuseros@mes.upv.es

Abstract

The information contained in this paper will be of interest not only to bridge engineers, but also to train manufacturers. The article provides practical insight into the degree of coverage of real *articulated trains* (ATs) that Eurocode EN1991-2 guarantees. In both the design of new railway bridges, as well as in the assessment of existing ones, the importance of a detailed knowledge of the *limits of validity* of *load models* cannot be overemphasised. Being essential components of the rail transportation system, the capacity of bridges to withstand future traffic demands will be determined precisely by the load models. Therefore, accurate definition of the limits of validity of such models reveals crucial when increased speeds and/or increased axle loads are required by transportation pressing priorities. The most relevant load model for a significant portion of the bridges in high-speed railway lines is the so-called HSLM-A model, defined in EN1991-2. Their limits of validity are described in Annex E of such code. For its singular importance, the effects of vibrations induced by HSLM-A are analysed in this paper with attention to the response of *simply supported bridges*. This analysis is carried out in a view to determine whether the limits of validity given in Annex E of EN1991-2 cover the largest part of cases of interest. Specifically, the vibration effects of HSLM-A are compared with those of the ATs described in such Annex E, and the response is analysed in depth for simply supported bridges, which are structures especially sensitive to passing trains at high speeds. New theoretical approaches have been developed in order to undertake this investigation, including a novel, simplified expression of the *train signature* for ATs that is convenient for its low computational cost. The mathematical proofs are included in the first part of the paper and two separate appendices.

load model, high-speed train, dynamic influence line, train spectrum, subresonance, higher-order resonance, bogie spectrum, bogie wheelbase, cumulative acceleration

Dynamic behaviour of bridges under critical articulated trains: Signature and bogie factor applied to the review of some regulations included in EN 1991-2

Pedro Museros1, Andreas Andersson2, Victor Martí3 and Raid Karoumi2

December 27, 2020

1 Introduction

In a way similar to the traditional approach adopted in Earthquake Engineering and other fields of Structural Dynamics, the idea of separating the action exerted by a train of loads —on a given structure— from the response of the structure itself has been exploited by a number of researchers in the past. This, in turn, has given rise to the appearance of different versions of the so-called *train spectra* over the last three decades.

Since the approach based on a train spectrum can be of interest for any vibration analysis related to railway vehicles, engineers and researchers concerned with the dynamic behaviour of track systems are one of the more active groups in this topic. In the early nineties Ford[**?**] discussed several questions related to the vibrations associated to the *sleeper passing effect*. In his paper, he presents the essential idea of combining the equal (but delayed) impulses produced by two axles (*i.e.* one bogie) on each sleeper, with the effect of two consecutive bogies placed under the same carriage. This combination results in the *spectrum of one single vehicle. i.e.* one single carriage resting on two bogies. The same idea was exploited later by Auersch[**?**] in a more comprehensive article, where random soil properties were also included for the analysis of the overall track/soil vibrations generated by high-speed trains.

Also of interest is the contribution from Krylov and Ferguson[**?**], where they suggested the possibility of supressing the vibrations created by each bogie by selecting a particular value of the bogie wheelbase. Implicitly, this idea is also pointed out by Ford[**?**] and Auersch[**?**] when they remark the existence of null values (*cancellations*) of the spectrum for particular relations of the wheelbase, speed and frequency. Similar strategies based on adjustable-size vehicles have been also proposed by Shin *et al.* [**?**].

More recently, one contribution from Milne *et al.* [**?**] emphasises that the most prominent peaks in the train spectrum correspond to frequencies close to integer multiples of the vehicle passing frequency. Moreover, Milne *et al.* indicate that the spectral peaks tend to integer multiples of the vehicle passing frequency as the number of vehicles increases. In coincidence with the findings from previous references[**?**],[**?**],[**?**], Milne *et al.* state that the magnitudes of such peaks are weighted by a function equivalent to the spectrum for a single vehicle, in such a way that the overall vibration level depends on the amplitude of vibration created by each single vehicle. In their article, Milne and his collaborators use the train spectra for suitable track engineering applications such as assessing the track modulus, or measuring the effective speed of passing trains.

When it comes to the analysis of structures subjected to the passage of railways, various groups of researchers have also resorted to the use of train spectra. Vestroni and Vidoli[**?**] published a versatile approach based on a nondimensional representation of the structural response and the Fourier Transform (FT) of the train loads. Their main aim was to give general expressions of useful bounds of the structural response at resonance, which they illustrated for both (i) a beam on elastic foundation and (ii) an arch bridge. They obtained manageable mathematical expressions when only one characteristic distance (carriage length) was considered, while numerical simulations were also presented for the case of two characteristic distances (carriage length and bogie wheelbase). Using this approach, the critical speeds were predicted and optimal speed ranges were derived for particular trains. Although being an innovative and rather general formulation, the mathematical tools presented by Vestroni and Vidoli were not exploited for the analysis of different train configurations, as it will be done here.

More recently, the train spectra of an ETR-1000 has been used by Matsuoka *et al.*[**?**] in conjunction with advanced numerical modelling and experimental measurements in order to analyse the level of local vibrations in an Italian viaduct subject to the passage of trains at speeds above 300 km/h. In their article, Matsuoka *et al.* endeavour to explain as well how higher-order resonances (*sub-resonance* phenomena) are responsible for the prominent contribution of *local modes*.

The most popular version of the train spectrum is, probably, the one introduced in year 1999 by the *European Rail Research Institute* committee D-214 (ERRI D-214) in the report RP6[**?**], which has had a determinant influence in the current European regulations[**?**]. Such spectrum, successfully named as the *train signature*, was derived both within the realm of the DER method (Decomposition of the Excitation at Resonance), as well as in the LIR method (Residual Influence Line). As regards the diffusion of such ideas in scientific publications, credit has to be attributed to Savin[**?**] in 2001, in a paper that disseminated the concept of the *signature* regarded as a sum of out-of-phase damped sinusoids of different amplitudes. This idea arises naturally also in other fields of sound and vibration theory as, for instance, the composition of decaying sounds that combine in some fragments of audio signals. However, due to the complex simultaneous treatment of such decaying sinusoids with the accompanying noise, they have been long since treated by means of different model fitting techniques[**?**].

In this article the equivalent concepts of train signature or train spectrum will be used in combination with the bogie spectrum (or *bogie factor*) for the critical assessment of standard load models. Particularly, attention will focus on the rational selection of critical *articulated trains* (ATs), *i.e.*, trains with car-bodies supported on shared (or *Jacobs*) bogies. Such kind of trains form the basis of one of the most important dynamic load models prescribed in EN1991-2[**?**] for the analysis of high-speed bridges: the so-called HSLM-A model.

The main objective of the paper is to analyse the conditions under which the HSLM-A model can be considered a safe upper bound of the actual, envisaged

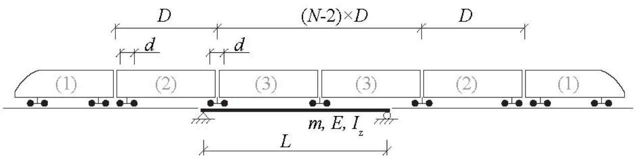

Figure 1: Scheme of an articulated train.

ATs that satisfy the limits described in *Annex E* of EN1991-2 (in what follows, simply *Annex E*). The importance of understanding such conditions can not be overemphasised: since the HSLM-A is presently used on a regular basis for the dynamic assessment of railway bridges in Europe, any actual bridge that is judged suitable for traffic at high (or increased) speeds will be *de facto* limited by the ranges of validity stated in Annex E. Consequently, any future AT that were not covered by the spectrum of the HSLM-A would be a potential candidate for creating vibration problems in particular structures. This, in turn, can be regarded as a limitation on the ranges of variation of design parameters that train manufacturers can explore for optimising their new vehicles in search of competitiveness, which has serious implications from an economic point of view.

Within the results presented in this paper, some cases will also be pointed out where strong vibrations could be expected at speeds that are not necessarily high (*i.e.*, speeds $V < 200\,\mathrm{km/h}$). Non-articulated trains will not be dealt with in this paper, but will be subject of forthcoming publications.

2 Closed-form expression of the (free) acceleration caused by a series of loads: Residual Influence Line

The intended audience of this paper comprises both railway bridge engineers and railway vehicle engineers. Since the latter may appreciate some previous background on bridge dynamics, Appendix A contains an brief summary of the main concepts regarding the analysis of railway bridges using the LIR method.

The general loading scheme of a series of coaches in an AT is well known and can be found, for instance, in EN1991-2[**?**]. A graphical description of such scheme of loads is presented in Figure **??**.

When a series of loads pass over a flexible structure, the effects caused by every moving load will add to those of the preceding loads. By neglecting vehicle-bridge interaction (VBI) and admitting that the system behaviour is linear, the maximum vibration level can be obtained by the principle of superposition in a most convenient manner. Such an approach was previously adopted in several investigations[**?**], and is a suitable departure point to analyse the critical combinations of load distances in a train.

Neglecting VBI can be regarded sometimes as an unwise, oversimplifying decision given the variety of sophisticated numerical models and software packages that can take VBI into account in the simulations. In this regard, it should be emphasised that VBI usually decreases the response predictions, but such "beneficial" effect depends markedly on the vehicle parameters[?]. For this reason, the definition of load models in regulations cannot rely on certain vehicle characteristics: if one load model depended on the level of VBI, *i.e.* on the values of the primary suspension stiffness, damping, semi-sprung mass, etc., then any modification introduced by vehicle manufacturers in such parameters, while still keeping the same or similar axle loads, could lead to the load model potentially not covering the dynamic effects of the new vehicles. Certainly, this situation would be undesirable.

Moreover, it should be recognised that the mechanical characteristics of railway vehicles can vary over the years for reasons related to passenger comfort, riding stability and other considerations related to vehicle design and performance, while the total axle loads may remain very similar, or even identical.

VBI can play an important role in the response of short or medium span bridges in certain cases, particularly when the degree of coupling between the primary suspension and the bridge is high[?]. In this regard, it would be convenient for bridge engineers to have a means of considering this factor in the regulations, but not through the load model itself due to the reasons explained above. Recently, one new simplified method has been proposed in an attempt to obtain an additional damping equivalent to the response reduction due to VBI effect[?].

In a view to compare the dynamic response induced by different load models based on *concentrated loads*, the VBI effect will not be considered in this paper. Conversely, load distribution due to the track and ballast, which is also an important factor for the prediction of bridge response[?], will be introduced in an appropriate way in order to analyse its influence on the results.

Focussing on the idea of applying the principle of superposition, it is clear that many different modes of vibration will be excited with different intensity when one single load travels over a flexible structure. In general, obtaining the combined response of all modes in a closed-form solution that is amenable to clear physical interpretation is not possible. Recently, Matsuoka *et al.*[?] have shown that local modes can as well have an influence in the total vibration response below 30 Hz, which is a reference frequency limit for bridge analysis[?]. Nevertheless, such local response has to be dealt with in a second level of approximation and is beyond the scope of this article. The analysis presented here is focussed on the structural response of bridges associated to their principal modes of bending deformation.

Once the free response of one of the modes is obtained under one passing load (either concentrated or distributed), superposition can be applied to get the total vibration amplitude. The same strategy can be applied to any type of structure, and can be exploited with special success if the total response is largely governed by the contribution of one single mode. Because this is especially the case when the peak vibration is due to resonance of one particular mode, the single mode approach can be useful in practical applications and has been used by many researchers: the DER and LIR methods rely on the contribution of the fundamental mode of simple beams[?], a similar approach was also adopted by Yang *et al.*[?], some extensive parametric studies have confirmed its suitability under different conditions[?],[?], and recently the approach has been extended to include the soil-structure interaction effect[?].

While some of the results and conclusions of this paper are valid for any kind of structure traversed by ATs, others will be particularized here for *simply* *supported bridges* (S-S bridges). The research works of ERRI D-214[**?**] some 20 years ago, as well as many other researchers since then, have pointed out such type of structures as being particularly sensitive to experiencing resonant vibration under high-speed traffic.

Let Γ_{max} be the maximum level of free vibration (acceleration) given by the fundamental mode of a flexible structure that is subjected to the passage of a unit concentrated or distributed moving load. Under the assumption of linear behaviour Γ_{max} will be proportional to the magnitude of the load, and will vary in some (probably non-monotonic) manner as a function of the speed of the load. It is also expected that Γ_{max} will be inversely proportional to some particular expression of the modal mass. It is usual to refer to Γ_{max} as the *Residual Influence Line*[**?**], or simply as the *Influence Line*.

The basic physical model of a S-S bridge used in this manuscript for dynamic analysis is the S-S beam. Both terms will be used equivalently as regards the mathematical formulations. For S-S beams of span L and constant cross-section with a small (viscous) damping ratio (typically $\zeta < 0.03$–0.05), the influence line of a unit, concentrated moving load has the well-know expression[**?**]

$\Gamma_{max} = 1mL/2 \cdot K1 - K^2 \cdot$
$\cdot \sqrt{1 + \mathrm{e}^{-\zeta\pi/K}(\mathrm{e}^{-\zeta\pi/K} + 2\cos(\pi K))}$

where m is the constant linear mass and K is the nondimensional speed of the first mode of vibration. For such fundamental bending mode, the nondimensional speed is a function of the span, the speed V and the fundamental period of vibration T:

$$K = VT2L \tag{1}$$

The influence line is then $\Gamma_{max} = \Gamma_{max}(mL, \zeta, K)$. The corresponding expression for highly damped beams can also be obtained in an analogous way[**?**].

The maximum vertical acceleration is often the governing variable in the design of short and medium span bridges in Europe, which is a consequence of the current Serviceability Limit States (SLS) prescribed in the regulations[**?**]. The LIR method allows to compute the maximum acceleration as the product of two terms:

$$a_{max} = \Gamma_{max}(mL, \zeta, K) \cdot G(F_i, d_i, \lambda, \zeta) \tag{2}$$

where the term $G(F_i, d_i, \lambda, \zeta)$ is the *train signature* or *train spectrum* and has the following form:

$\mathrm{G} = \sqrt{\left(\sum_{i=1}^{k} F_i\theta_i \cos(2\pi\delta_i)\right)^2 + \left(\sum_{i=1}^{k} F_i\theta_i \sin(2\pi\delta_i)\right)^2}$
$\theta_i = \mathrm{e}^{-\zeta 2\pi\delta_i}$
$\delta_i = d_k - d_i\lambda$
$\lambda = VT$

In equation (**??**), k is the total number of loads in the train and every d_i(m) distance associated to each load F_i(kN) is usually measured from the first load, in such a way that $d_1 = 0$. Because the end passenger coaches and the power cars break the repetitive pattern of load distances formed by the sequence of intermediate passenger cars, the possibility exists that the maximum response does not occur precisely when the last load leaves the bridge; therefore, equation (**??**) has to be applied for all possible *subtrains* that start at the first axle load, and then retain the maximum value that has been computed among the subtrains[?].

3 Closed-form expression of the (free) acceleration caused by a series of coaches with shared bogies (*articulated coaches*)

The decomposition given by equation (??) permits to focus on the effects of the train of loads, given that the first factor Γ_{max} does not depend on the loads. Moreover, most of the essential conclusions derived from the analysis of the signature $G(F_i, d_i, \lambda, \zeta)$ can be obtained without reference to damping, with the exception of the amplitude levels.

In a first stage, the power cars will not be considered because the distances between their loads do not follow a regular pattern in comparison with the passenger cars, and therefore obtaining a closed-form solutions amenable to interpretation becomes infeasible due to the simultaneous dependence on too many parameters. Therefore, the scheme of Figure **??** is adopted, but without locomotives. The characteristic length of the coach is D, while the bogie wheelbase is b. In EN1991-2[?], the bogie wheelbase is referred to as d_{BA}, but instead $b = d_{BA}$ is used in what follows for the sake of conciseness.

In the rest of the paper, symbol k will refer to the number of bogies, which, in turn, is one unit more than the number of cars n_c: $k = n_c + 1$. Therefore, the total number of loads is $2k$. All loads are considered to have the same value, and thus $F_i = F$ is the constant axle load.

In order to arrive to a correct physical insight, the signature will be next decomposed into two factors. An additional assumption is that all passenger cars are of equal length D while, in reality, the initial and final cars (number (2) in Figure **??**) will be somewhat shorter. With these hypotheses, the main objective of this section is to analyse the sequence of bogies in the coaches, *i.e.* the selection of critical combinations of D and b.

3.1 Decomposition of the signature of a series of coaches with shared bogies (*Articulated Train*)

The effects of two consecutive loads in one bogie will be gathered into a single function that will take values between two (perfect in-phase addition, or *bogie resonance*) and zero (perfect *bogie cancellation* by destructive addition of the effects of each axle). This will be the spectrum or signature of the bogie f_B.

Then, the series of vibrations generated by each pair of loads in one bogie, each of them of amplitude proportional to $F \cdot f_B$, ought to be combined by realizing that they create a repetitive sequence of k bogies at equal distances D. This is equivalent to obtaining, from equation (??), the particular expression of the damped signature of a set of k equidistant unit loads. In previous works such expression was obtained only for resonant speeds[?]. In the following section, this result is generalised in a new closed-form expression that is valid both for resonant and non resonant speeds. Since this expression includes the effects of structural damping, the graphical representations are similar to the ones from Milne *et al.*[?] but the effect of the decaying oscillations are shown.

3.2 Signature of a series of equidistant loads (*Regular Train*)

Choosing suitable nondimensional parameters is important for subsequent graphical representation and interpretation. The following nondimensional wavelength is defined for convenience[?]:

$$\Lambda = \lambda/D = VT/D \tag{3}$$

The nondimensional wavelength Λ represents the fraction of D travelled in one period of the free vibration. Also, an auxiliary parameter is defined that increases with damping:

$$\sigma = e^{\zeta 2\pi/\Lambda} \geq 1 \tag{4}$$

The following mathematical expression of the *signature* of a set (train) of k equidistant unit loads that travel at distance D is a contribution of this article and is derived in Appendix B. Its simplified expression is

$$\begin{aligned} G_E(k,\Lambda,\zeta) &= k \qquad \text{if } \zeta = 0 \ \text{ and } \ \Lambda = 1, 1/2, 1/3, ... \\ G_E(k,\Lambda,\zeta) &= \sqrt{\sigma^{2(1-k)} f_k(\sigma,\Lambda) f_1(\sigma,\Lambda)} \qquad \text{otherwise.} \end{aligned} \tag{5}$$

where

$$f_k(\sigma,\Lambda) = (1 + \sigma^{2k} - 2\sigma^k \cos(2k\pi/\Lambda)) \tag{6}$$

and $f_1 = f_k(k=1)$. It is apparent that ratio Λ equals to one will produce resonant addition of the effects of consecutive loads, while ratios Λ equal to 1/2, 1/3, etc., will produce sub-resonance. In different contexts, ratio $\Lambda = 1/j, j = 1, 2, 3\ldots$ is referred to as the jth resonance, jth sub-resonance, or also jth sub-harmonic. As equation (**??**) shows, in absence of damping the maximum peaks will be of equal value $G_E = k$ for every sub-harmonic. Figure **??** displays the signature for a set of 15 loads. The evolution of G_E for $\Lambda > 1$ is of little practical relevance in actual railway bridges and is discussed in Appendix B.

The maximum peaks in Figure **??** are obtained for $\Lambda = 1, 1/2, 1/3, \ldots$, where equation (**??**) simplifies as follows[?]:

$$G_E(k, \Lambda = 1/n, \zeta) = \mathrm{e}^{2\pi n\zeta} - \mathrm{e}^{-2\pi n\zeta(k-1)}\mathrm{e}^{2\pi n\zeta} - 1, \quad n = 1, 2, \ldots \tag{7}$$

Equation (**??**) is a suitable basis to interpret the influence of damping and the number of loads on the signature peaks. When k is very high, the second term in the numerator of equation (**??**) tends to vanish and the maximum G_E is obtained. This value is shown in Tables **??** and **??** for the different sub-resonances and seven levels of damping, where $G_{E,max}$ is indeed an asymptotic value that provides a measure of the maximum expected intensity of each sub-resonance. Because in certain cases $G_{E,max}$ will only be reached by trains containing a very large number loads, it is of interest to know how many loads would be required to exceed three reference thresholds: 50%, 75% and 90% of $G_{E,max}$. Such values are also presented in Tables **??** and **??**. As an example, it is shown in Tables **??** and **??** that an AT with, say, 15 equidistant bogies, is capable

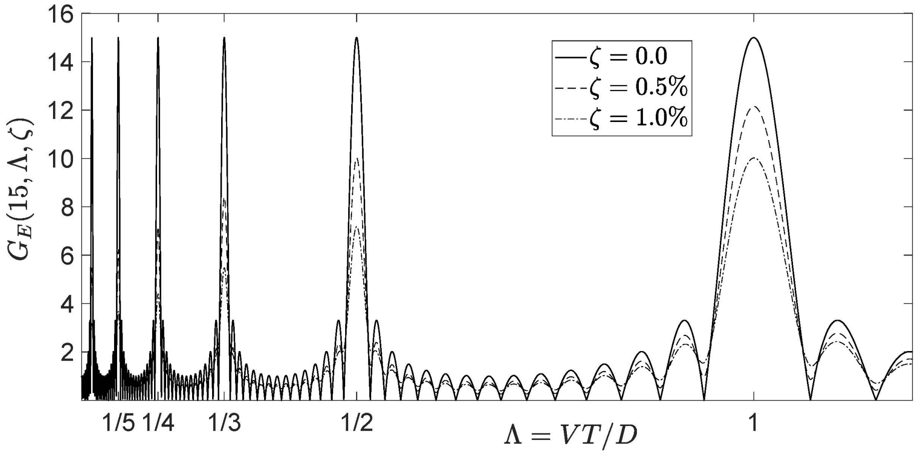

Figure 2: Signature or spectrum of a set of $k = 15$ equidistant, concentrated unit loads.

	$\Lambda = 1$				$\Lambda = 1/2$				$\Lambda = 1/3$			
ζ	$G_{E,max}$	$k_{50\%}$	$k_{75\%}$	$k_{90\%}$	$G_{E,max}$	$k_{50\%}$	$k_{75\%}$	$k_{90\%}$	$G_{E,max}$	$k_{50\%}$	$k_{75\%}$	$k_{90\%}$
0.50%	32.3	23	45	74	16.4	12	23	37	11.1	8	15	25
0.75%	21.7	15	30	49	11.1	8	15	25	7.59	5	10	17
1.00%	16.4	12	23	37	8.47	6	12	19	5.82	4	8	13
1.25%	13.2	9	18	30	6.88	5	9	15	4.76	3	6	10
1.50%	11.1	8	15	25	5.82	4	8	13	4.06	3	5	9
1.75%	9.60	7	13	21	5.07	4	7	11	3.56	3	5	7
2.00%	8.47	6	12	19	4.50	3	6	10	3.18	2	4	7

Table 1: Representative values of G_E and number of loads k required to exceed 50%, 75% and 90% of $G_{E,max}$.

of fully building up (90%) the second sub-resonance ($\Lambda = 1/2$) for damping 1.25% or higher, as well as the third sub-resonance ($\Lambda = 1/3$) for damping around 0.875% or higher; also it will build up at 50% all sub-resonances, except for the first one if damping were very light.

An interesting conclusion that can be drawn from Tables **??** and **??** is that bridges where damping is above some 1.5–2.0% need not be traversed by very long trains to build up resonance to its maximum achievable amplitude (for such train type and bridge): the bottom rows for columns $\Lambda = 1/2$ or smaller show that with $5 - 10$ loads resonance is build up to 90%.

3.3 Bogie factor f_B

The following nondimensional parameters are defined that will be convenient in what follows:

$$\mu = \lambda/b = VT/b$$

ζ	$\Lambda = 1/4$ $G_{E,max}$	$k_{50\%}$	$k_{75\%}$	$k_{90\%}$	$\Lambda = 1/5$ $G_{E,max}$	$k_{50\%}$	$k_{75\%}$	$k_{90\%}$	$\Lambda = 1/6$ $G_{E,max}$	$k_{50\%}$	$k_{75\%}$	$k_{90\%}$
0.50%	8.47	6	12	19	6.88	5	9	15	5.82	4	8	13
0.75%	5.82	4	8	13	4.76	3	6	10	4.06	3	5	9
1.00%	4.50	3	6	10	3.71	3	5	8	3.18	2	4	7
1.25%	3.71	3	5	8	3.08	2	4	6	2.66	2	3	5
1.50%	3.18	2	4	7	2.66	2	3	5	2.31	2	3	5
1.75%	2.81	2	4	6	2.36	2	3	5	2.07	2	3	4
2.00%	2.53	2	3	5	2.14	2	3	4	1.89	1	2	4

Table 2: Representative values of G_E and number of loads k required to exceed 50%, 75% and 90% of $G_{E,max}$.

$$\eta = D/b = \mu/\Lambda \tag{8}$$

The ratio $\eta = D/b$ is of particular importance since the range of validity of the HSLM-A is restricted to *not close to integer* values of η, as it will be discussed later.

No definite trends exist that link the actual values of coach length D of ATs in the range $[18, 27]$m to the bogie wheelbase b. Both are key parameters that are selected by vehicle manufacturers in order to maximize its dynamic performance. Doménech *et al.*[?] found relations between the coach length and the *wheelbase between bogies* ($D - d_{BS}$ in Annex E) in conventional carriages, but no actual relations of D with the bogie wheebase. Moreover, in one background document from ERRI Committee D-214.2[?], where the basis of design of the HSLM-A are described in detail, no relation is established between b and D. Following such document[?], in this article it is assumed as a reasonable hypothesis that D values in the range $[18, 27]$m can coexist with $b \in [2.5, 3.5]$m. This, in turn, leads to a range $\eta \in [5.14, 10.8]$.

If the general expression of the signature given by equation (**??**) is particularized for values $F_i = 1$, $k = 2$, $d_1 = 0$, $d_2 = b$, straightforward operations lead to the expression of the bogie factor:

$$f_B(b, \lambda, \zeta) = \sqrt{1 + e^{-\zeta 4\pi b/\lambda} + 2e^{-\zeta 2\pi b/\lambda} \cos(2\pi b/\lambda)} \tag{9}$$

Such expression can also be written as a function of μ, to be used in equation (**??**) in next section:

$$f_B(\mu, \zeta) = \sqrt{1 + e^{-\zeta 4\pi/\mu} + 2e^{-\zeta 2\pi/\mu} \cos(2\pi/\mu)} \tag{10}$$

As it was mentioned in the introductory section, the concept of bogie spectrum is not a new one. However, it will be expressed next in a manner suitable for arriving to some useful conclusions. Indeed, *spectrum* is a term that is more

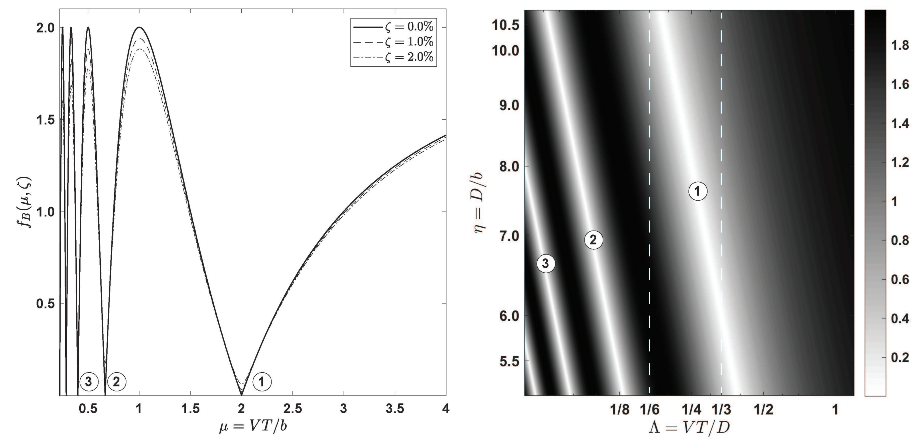

Figure 3: Bogie factor f_B as a function of μ and ζ (left), or Λ and η for $\zeta = 0$ (right, in log-log axes).

often linked to frequency dependence, and therefore bogie *factor* will be used preferably. Given the relation between μ, Λ and η, the bogie factor can be rewritten as

$\mathrm{f}_B(\Lambda, \eta, \zeta) =$
$\sqrt{1 + e^{-\zeta 4\pi/(\Lambda\eta)} + 2e^{-\zeta 2\pi/(\Lambda\eta)} \cos(2\pi/(\Lambda\eta))}$

The bogie factor is always comprised between zero and two. If damping is neglected, one of its possible expressions is as follows:

$$f_B(\Lambda, \eta, \zeta = 0) = \sqrt{2\,(1 + \cos(2\pi/(\Lambda\eta)))} \qquad (11)$$

The bogie factor can be plot in different manners. Figure **??** shows two of them: one is a function of μ for different values of damping, and the other is a contour log-log plot as a function of Λ and η for the undamped case. The cancellation by addition points (or lines) (1), (2), (3) ($f_B(\zeta = 0) = 0$) can be obtained from equation (**??**), as well as the maximum points (or lines):

Cancellations: m = 1,2,. . .
$\mu = 22m - 1 \iff \eta = 2/\Lambda 2m - 1$

Maxima (*bogie resonance*): m = 1,2,. . .
$\mu = 1m \iff \eta = 1m\Lambda$

In Figure **??** [left], f_B tends monotonically to 2.0 for increasing values $\mu > 2$. The same phenomenon is observed in Figure **??** [right], in the region to the right of the first cancellation line (1). Bogie cancellations are caused by addition of out-of-phase vibrations. Besides, in Figure **??** [right] it can be seen that sub-harmonics $\Lambda = 1/8$ and above are always located above the second bogie cancellation (2), which encompasses the vast majority of cases of interest.

An important thing to notice in Figure **??** [right] is that f_B varies in a smooth monotonic fashion with η, in coincidence with the resonant cases for the sequence of carriages: $\Lambda = 1, 1/2, 1/3 \ldots$. Such fact is apparent for $\Lambda = 1$ and $\Lambda = 1/2$, but also for $\Lambda = 1/3$ once the cancellation (1) is exceeded (see the right dashed vertical line). Also for the rest of resonant values of Λ, such as

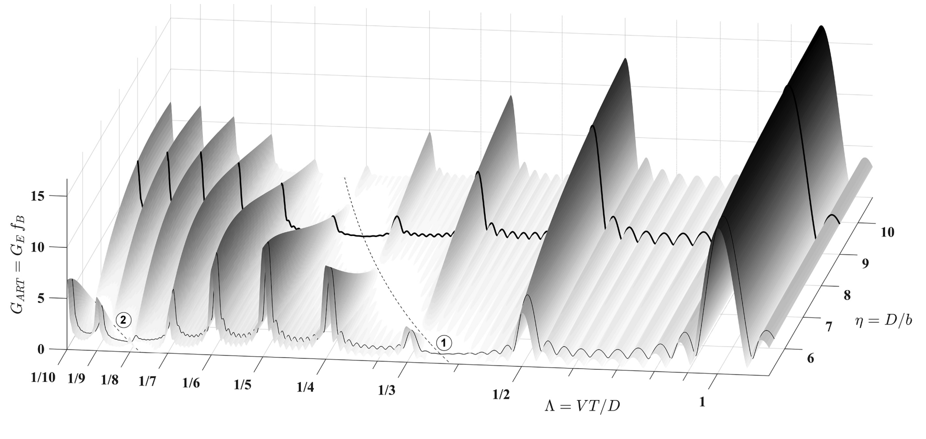

Figure 4: Signature of a series of $k-1=9$ articulated coaches with unit loads and damping $\zeta = 0.5\%$. Log axis in Λ

1/6 (see the left dashed vertical line), $f_B(\Lambda, \eta)$ varies smoothly, featuring values $f_B(1/6, 6.0) = 2.0$; $f_B(1/6, 6.5) = 1.94$; $f_B(1/6, 7.0) = 1.80$; $f_B(1/6, 7.5) = 1.62$. Therefore, from a physical point of view, there is no reason to think that ratios $\eta = D/b$ close to an integer will produce a dynamic effect that is significantly larger than those corresponding to D/b not close to an integer. Even if such integer $D/b = D/d_{BA}$ ratios are specifically left out of the range of validity of HSLM-A in Annex E, the reasons for such a condition are not supported by the present results.

3.4 Signature of a series of coaches with shared bogies (*Articulated Train*)

One further evidence of the preceding statement regarding the D/b ratios is given by the combined plot of Figure **??** multiplied by Figure **??** [right]. This product is precisely the signature of the series of $(k-1)$ articulated coaches, *i.e.* k bogies with equal forces F. Figure **??** shows a 3D view of such comprehensive train spectrum for $k = 10$ and $F = 1$. The general mathematical expression of it is obtained by multiplying equation (**??**) times either equations (**??**) or (**??**):

$$G_{\text{ART}}(k, \Lambda, \eta, \zeta) = G_E(k, \Lambda, \zeta)\, f_B(\Lambda, \eta, \zeta)$$

$$G_{\text{ART}}(k, \Lambda, \mu, \zeta) = G_E(k, \Lambda, \zeta)\, f_B(\mu, \zeta)$$

The signature given in equations (**??**) or (**??**) is a good approximation to the general signature from equation (**??**) in the case of ATs. Figure **??** shows the comparison of both for an ensemble of 1001 trains that cover the ranges of Annex E with $D \in [18, 27]$m in steps of 0.1 m, and $b \in [2.5, 3.5]$m in steps of 0.1 m. The lengths of such ATs are adjusted to be as close as possible but no longer than $L_{tot} = 400$ m while keeping the total weight below $P_{tot} = 10\,000$ kN, which are conditions stipulated in Annex E. Besides, the power cars are identical to the ones of the HSLM-A model. Such three criteria (total length $< L_{tot}$, total weight $< P_{tot}$, power cars equal to HSLM-A) are hold for all ATs derived from Annex E that will be analysed in this paper. The step for the wavelength is 0.01 m. No subtrains need to be considered for the simplified signature.

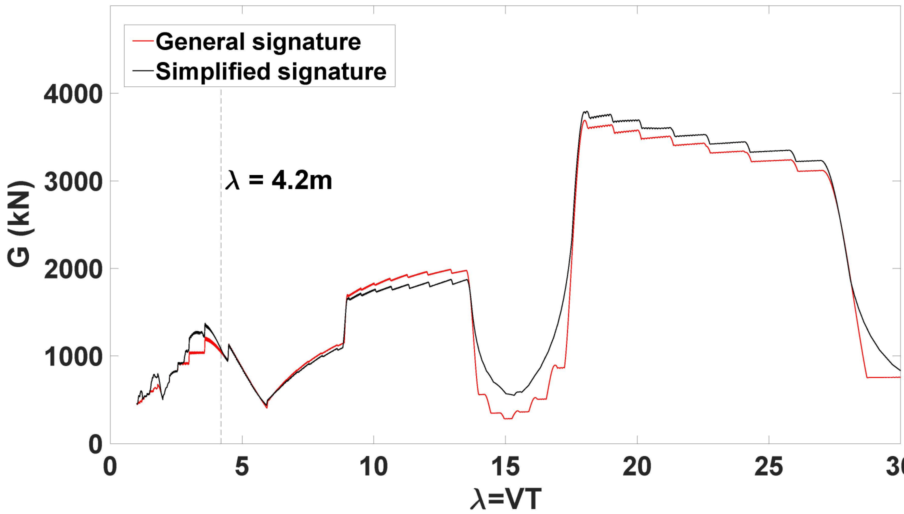

Figure 5: Signature of the Annex E articulated trains for damping $\zeta = 1\%$.

As it can be seen in Figure ??, the agreement is very good for wavelengths $\lambda > 4.2\,\mathrm{m}$: the first resonances are slightly underestimated, while the second ones are slightly overestimated. For short bridges where the dominant wavelengths can be short the simplified signature will not be useful because the expected relative error is too large. Conversely, the simplified signature will be convenient for parametric studies during preliminary design stages providing that the dominant wavelength is larger than 4.2 m. It should be emphasised that the computational cost of the simplified signature is one order of magnitude less than that of the general one.

In a way analogous to Figure ??, Figure ?? compares the general signature of HSLM-A model, for $\lambda > 4.2\,\mathrm{m}$ and 1% damping, with the simplified signature. In this case two extra cars have been added to the simplified signature in order to have a better fit of the first and second sub-resonances of each train.

If the signature given in equations (??) or (??) is finally multiplied by the influence line given by equation (??), the maximum acceleration in free vibration is obtained, which is a good estimate in cases when one mode is predominant and the structure is short in comparison with the train length. Thus, equation (??) can be rewritten finally as

$$\mathrm{a}_{max} = \Gamma_{max}(mL, \zeta, K) \cdot G_{\mathrm{ART}}(k, \Lambda, \eta, \zeta)$$
$$= \Gamma_{max}(mL, \zeta, K) \cdot G_E(k, \Lambda, \zeta) \cdot f_B(\mu, \zeta)$$

In what follows the particular expression adopted for Γ_{max} in equation (??) is that for S-S beams, which depends on the total mass mL. This strategy can of course be adapted to beams on elastic supports, plate-like bridges, etc.

As it can be seen clearly from Figure ??, the peak load combination effects take place always in correspondence of $\Lambda = 1/n$, *i.e.* when resonance associated to distance D takes place. The maximum values of G_{ART} in Figure ?? would be 20 in absence of damping. Notice that G_{ART} is to be multiplied by F (kN). No abrupt or singular resonant effect is observed for integer values of the D/b ratio. Therefore, integer values of η can not be retained as being particularly

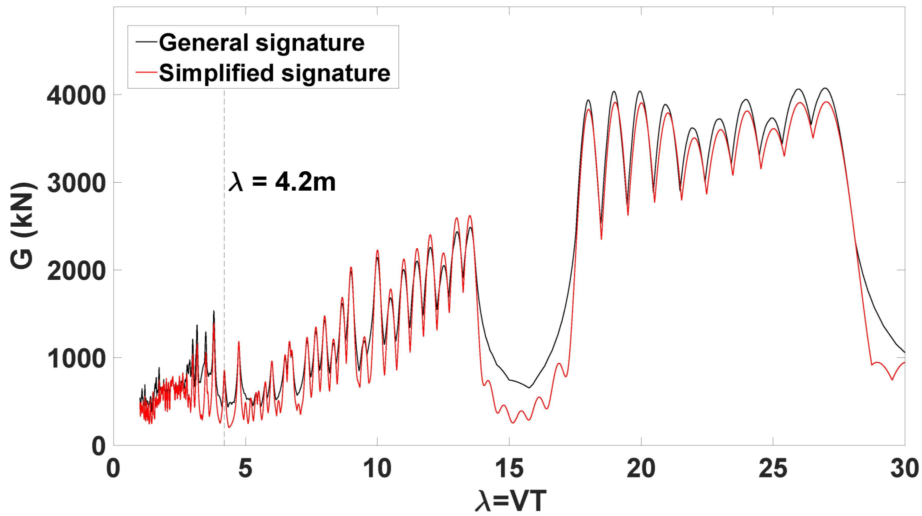

Figure 6: Signature of the HSLM-A model for damping $\zeta = 1\%$. Two extra cars added for the simplified signature.

harmful from the point of view of vibrations.

Based on equation (??), Figure ?? offers additional insight on the effect of the D/b ratio. Such figure is the counterpart of Figure ??, but has been plotted as a function of μ instead of η (damping neglected for the sake of clarity). For the purpose of illustration, the point of coordinates $(\Lambda, \mu) = (1/6, 1)$ represents that each cycle of bridge vibration is of the same duration as one bogie passage, while the passage of one single carriage will last six times as much. The logarithmic scale in both axes produces inclined parallel lines for each value of $\eta = D/b$. Three of such lines are plotted for values $\eta = 18/3.273 \simeq 5.5$ (dotted line), $\eta = 18/3 = 6$ (continuous line) and $\eta = 18/2.769 \simeq 6.5$ (dash-dotted line). For most of the sub-resonances, the maximum values of the signature correspond to the dotted or dash-dotted lines, for which the η ratio is as far as possible from being integer. Even in the case where theoretically it can be predicted (see equation (??)) that a maximum effect is expected for $\eta = 18/6 = 3$, which is precisely $\Lambda = 1/6$, the value of the bogie factor is 1.92 for the dash-dotted line, 2.0 for the continuous line and 1.94 for the dotted line. Because the same proportions will hold for the signature according to equation (??), it is clear that the integer η ratio is not significantly more aggressive.

4 Analysis of the HSLM-A load model

4.1 Existence of particular cases of interest

In Figure ?? two black lines are included of constant η ratio: the thicker one corresponds to the η ratio of train HSLM-A1: $18/2 = 9$; the thinner line corresponds to HSLM-A2: $19/3.5 = 5.43$. As it can be seen, HSLM-A1 produces strong vibration levels for the first two resonances, but lower for the third and

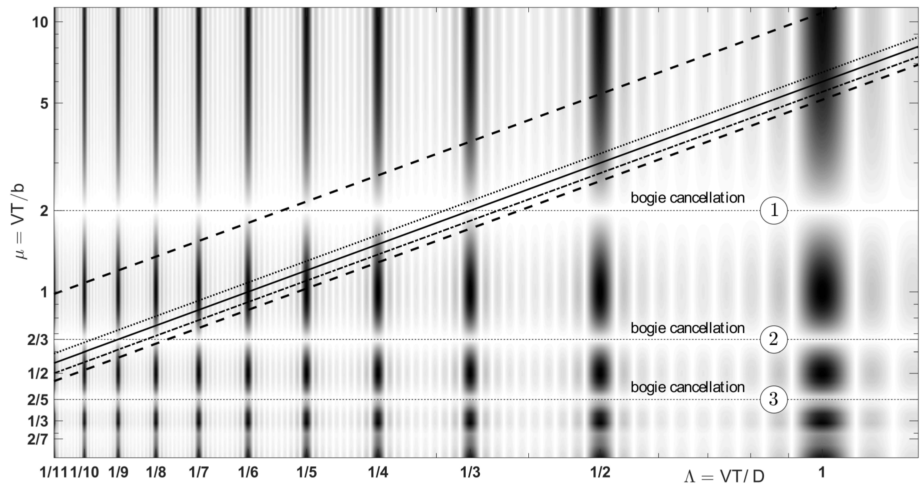

Figure 7: Contour plot of the undamped signature of a series of $k-1=9$ articulated coaches, as a function of D-nondimensional wavelength (Λ) and b-nondimensional wavelength (μ). Extreme dashed lines correspond to η limits for Annex E articulated trains.

even very low for the fourth and fifth resonances. HSLM-A2 produces rather low levels in the second resonance and very low ones in the third resonance, but on the other hand it is optimal for the fourth and fifth sub-harmonics.

Because of this influence of the bogie wheelbase in the dynamic effects created by one train, ERRI D-214.2[**?**] carried out a comprehensive parametric study with a view to optimize the maximum response of the 10 HSLM-A trains by varying both b and F. The final result is the load model included in EN1991-2, where axle loads up to 210 kN are used, as well as exceptionally short bogies of $b=2.0$ m. However, the range of validity of HSLM-A is restricted in Annex E to trains with axle loads not higher than $P_{\text{ref}}=170$ kN, and bogie wheelbases $b\in[2.5,3.5]$m. What was the reason why ERRI D-214.2 used higher axle loads and shorter bogies than the Annex E limits? Most likely, because that was a rather clean and simple means of producing a load model that can cover real trains by using only 10 articulated trains, which is convenient for dynamic analyses in practical engineering applications.

The question that arises from there is whether it is possible or not to find cases where the selection of b done by ERRI D-214.2[**?**] was not optimal. If this were so, would it be possible to find ATs that exceed the vibrations created by HSLM-A model, while still satisfying the range of validity in Annex E? The answer to such question is affirmative, but yet it needs to be nuanced and discussed in different scenarios. As a starting point, one example of an Annex E train that is not covered by HSLM-A is discussed next.

Figure **??** shows the response of a bridge of span $L=21.0$ m, where the HSLM-A model is compared to one “real” AT derived from Annex E. Only the fundamental mode is included in the simulation of the (Bernoulli-Euler) bending deformation. The values adopted for the mass, damping and natural frequency are realistic ones for a composite bridge. Load distribution is not yet taken into account in this example.

It should be recalled that the emphasis of the article is in the comparison of load models, and therefore it is important to avoid including features in the structural model that may depend on the end user implementation, such as the modelling of the track, bearings, etc. Also, track irregularities are not considered since the EN1991-2 prescribes them (φ'') as a function of the bridge span and frequency regardless of the load model. The sampling time step used is $dt = T/20$ for the closed-form time integration of the differential equation of motion. Speed increment is equal to 0.5 km/h.

The real train is of the articulated type, with $F = P_{\text{ref}} = 170\,\text{kN}$, $D = 19\,\text{m}$ and $b = 2.5\,\text{m}$. The peak mid-span response at 188 km/h is 5.01 m/s^2, and exceeds the maximum values of HSLM-A1 and HSLM-A2 by 42%. This exceedance is due to the somewhat low effects of HSLM-A2 at the second sub-resonance, which is a consequence of its long bogie wheelbase $b = 3.5\,\text{m}$. When three modes are included in the analysis the results are only slightly different, with peak values for certain HSLM-A trains that increase some 12%, but the peak of the real train increases also and the exceedance is still of almost 30%.

Now, in order to assess the relevance of such kind of cases, the *exceedance* in acceleration is defined for each speed V as

$\Delta a(V) =$

$\max\left[100\, a_{max,\text{REAL}}(V) - a_{max,\text{HSLMA}}(V) a_{max,\text{HSLMA}}(V) \quad ; \quad 0\right]$

However, it should be recalled that in EN1991-2[?] the following relation between the design and nominal speeds is established: "1.4.3.7. *Maximum Nominal Speed* [$= V_{\text{nom}}$]: generally the Maximum Line Speed at the Site [...] 1.4.3.8 *Maximum Design Speed* [$= V_{\text{max}}$]: generally $V_{\text{max}} = 1.2\, V_{\text{nom}}$".

The question that arises from there is the following: is an exceedance Δa of the kind shown in Figure **??** relevant for the assessment of bridges based on HSLM-A model? Two different situation can be distinguished.

One case analogous to the one in Figure **??** would not be relevant because the design speed to be used with HSLM-A is $V_{\text{max}} = 1.2\, V_{\text{nom}}$. Therefore, even if the real train reaches its non-covered peak at 188 km/h, the HSLM-A should be analysed up to, at least $1.2 \cdot 188 = 225.6$ km/h. Figure **??** shows that, in such case, train A3 for $V > 198$ km/h, and train A5 for $V > 217.8$ km/h would be decisive for the design (in what follows we will refer to such determinant trains as the *governing trains*).

It is of interest, then, to define the *speed increase required for HSLM-A to cover a real train* ΔV as the minimum difference in speed (as a percentage) that is needed to reach, from the dominant peak of the real train, the response curve of the HSLM-A with identical amplitude, but at higher speed (the concept is illustrated in Figure **??**). If $\Delta V \leq 20\%$, the exceedance Δa is not relevant. Conversely, the situation becomes relevant when $\Delta V > 20\%$.

Also, some values of exceedance Δa below certain tolerance limits will not be considered relevant, as it will be discussed later.

It should be noticed that all phenomena described in relation to Figure **??** take place at speeds below 200 km/h, which is a range of speeds not usually considered of risk in dynamic analysis. However, this is only a consequence of the bridge frequency being 5.5 Hz; if the frequency were only above 5.9 Hz, the same phenomena would take place at speeds greater than 200 km/h.

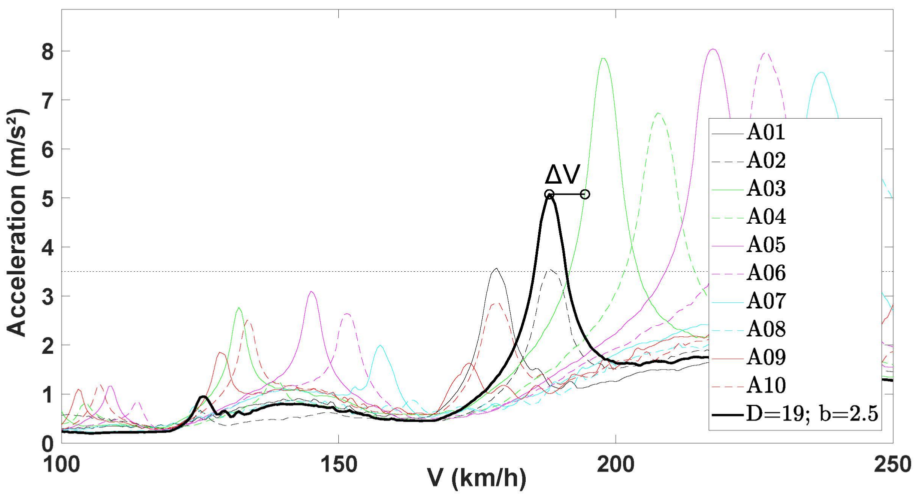

Figure 8: Maximum acceleration at mid-span in a simply supported bridge defined by: $L = 21.0\,\mathrm{m}$, $m = 16\,000\,\mathrm{kg/m}$, $f = 5.5\,\mathrm{Hz}$, $\zeta = 0.6\%$.

4.2 Theoretical prognosis of critical cases

The case described in Figure **??** was predicted from the theoretical expressions given by equations (**??**), in a preliminary screening of span lengths equal to integer values from 7 to 30 m. In order to do so, one key point is to realize that, in Figure **??**, each sub-resonance requires a particular value of η for f_B being maximum, which leads also to a maximum G_{ART}. This means that the values of b can be optimised for every D and every $\Lambda = 1/n$. If this optimisation is carried out, the potential increase obtained for G_{ART}, in correspondence of each n*th* sub-resonance and each i*th* HSLM-A train, can be summarised into a matrix $\left[f_B^{\Delta}\right]$. When the values in such matrix are greater than one, this means that the bogie wheelbase $b_{\mathrm{HSLMA},i}$ of the i*th* HSLM-A is not optimal for $\Lambda = 1/n$:

$$f_{B,in}^{\Delta} = \max\left\{f_B\left(\Lambda = 1/n, \eta \in \eta_{range}, \zeta\right)\right\} \rho_i\, f_B\left(\Lambda = 1/n, \eta = \hat{\eta}_i, \zeta\right)$$

$$\begin{aligned} \eta_{range} &= [18/3.5, 27/2.5] = [5.14, 10.8] \\ \rho_i &= P_{\mathrm{HSLMA},i}/P_{\mathrm{ref}} = P_{\mathrm{HSLMA},i}/170\,\mathrm{kN} \\ \hat{\eta}_i &= D_{\mathrm{HSLMA},i}/b_{\mathrm{HSLMA},i} \\ \zeta &= 0 \\ i &= 1, 2, \ldots 10 \\ n &= 1, 2, \ldots \end{aligned} \qquad (12)$$

Damping is set to zero in equation (**??**) because Figure **??** shows that its effect is very small in the range of interest. Matrix $\left[f_B^{\Delta}\right]$ is represented in Table **??** for $n \leq 6$, where it should be emphasised that the numerator $\max\left\{f_B\left(\Lambda = 1/n, \eta \in \eta_{range}, \zeta\right)\right\}$ in equation (**??**) is restricted to real trains that are theoretically covered by HSLM-A, according to Annex E. If the values of $\left[f_B^{\Delta}\right]$ are less than or equal to one, they are of no practical interest and

	$\Lambda=1$	$\Lambda=1/2$	$\Lambda=1/3$	$\Lambda=1/4$	$\Lambda=1/5$	$\Lambda=1/6$
A1	–	–	–	4.41	5.74	2.00
A2	–	1.43	1.68	–	–	–
A3	–	–	–	1.80	A3 cancels	3.06
A4	–	1.05	1.74	2.01	1.24	–
A5	–	–	–	–	5.63	6.96
A6	–	–	–	–	3.39	13.33
A7	–	–	–	–	2.28	A7 cancels
A8	–	–	–	–	A8 cancels	2.54
A9	–	–	–	–	1.18	5.53
A10	–	–	–	–	–	3.57

Table 3: Matrix $\left[f_B^{\Delta}\right]$ of potential increases in resonant response of *real trains* with reference to HSLM-A effects.

are shown as a hyphen (–). Cancellations of the bogie factor of some HSLM-A trains lead to an infinite increase and are mentioned explicitly.

Table **??** shows that in some cases the effect of particular HSLM-A trains is indeed smaller than the effect of the real trains. For instance, $f_{B,14}^{\Delta}=4.41$ and $f_{B,22}^{\Delta}=1.43$. Also, many values in the table are larger than one for the $5th$ and $6th$ sub-resonances.

However, all of the cases where $f_{B,in}^{\Delta}>1$ are not effectively relevant, for the following reasons: (i) the power cars can have an effect which is particularly significant when resonance occurs for the higher coach length sub-harmonics $\Lambda=1/4,1/5,\ldots$; (ii) the third sub-resonance of train A10 coincides with the second one of train A1 and, at speeds below the third sub-resonance of A4, the various sub-resonances of the different trains intermingle and make it difficult to know a priori which one will be predominant; (iii) it should be realised that point (ii) is even more involved because the different span lengths will lead to cancellation of the influence line Γ_{max} in particular speeds, and therefore some prominent peak may disappear despite being very noticeable in the train signature. Therefore, Table **??** gives hints about where to look at, but can not provide a definitive answer. Such an answer is to be searched with a more comprehensive study as described next.

5 Parametric analyses of the level of exceedance of HSLM-A

Due to the reasons explained in the previous section, examples can be found where the bogie wheelbases of the HSLM-A trains are not optimised for all sub-resonances. Therefore, in order to assess the validity of the HSLM-A under relevant conditions, a series of parametric analyses have been carried out. The hypotheses of such analyses are the following:

- The characteristics of the physical model are the ones described in the section entitled *Existence of particular cases of interest.* Two different methods for computing the vertical acceleration are considered, namely

(i) the general signature in equation (**??**), and (ii) the time integration of the equations of motion. The simplified signature will not be used because wavelengths below 4.2 m will be also involved.

- Only S-S bridges on rigid supports are analysed.

- Load distribution is introduced by means of the wavelength-dependent distribution factor derived by ERRI D-214[**?**] and adopted by the UIC[**?**]. Recent studies have shown that such ERRI-UIC distribution factor is slightly conservative in comparison with a triangular distribution with a total length of 3 m[**?**] which, in turn, was proposed as a good approximation to the actual load spreading effect due to ballast by Axelsson *et al.*[**?**].

- The HSLM-A model is considered to cover the effects of Annex E trains if the exceedance in acceleration Δa, as defined by equation (**??**) is smaller than some particular limit Δa_{lim}. Such limit should correspond to the fraction of the global safety coefficient of the structure that bridge engineers would accept as being "consumed" by exceeding the load (HSLM-A) model. Assigning an indisputable value for Δa_{lim} would require a comprehensive approach that is beyond the scope of this paper. As a reference, a value $\Delta a_{lim} = 10\%$ was adopted by ERRI D-214.2 for validating the applicability of HSLM-A to continuous bridges[**?**]. However, higher values up to at least 15% will also be explored in order to assess the problem from an engineering point of view.

- The maximum governing response is computed in the sense of the *cumulative maximum acceleration.* Obtaining the cumulative maximum in a range of speeds implies that, given a peak response of amplitude a_0 that corresponds to speed V_0, response levels $a \leq a_0$ are disregarded for every higher speed $V > V_0$. This entails an evaluation of the maximum response in a way similar to the *rainflow counting method* used for fatigue analysis, and is justified by considering that if a train reaches a maximum nominal speed V_{nom} at one site, it is always possible that the same train will circulate in some moment at a lower speed due to particular circumstances in the line.

- The real trains derived from Annex E have $D \in [18, 27]$m in steps of 0.5 m, and $b \in [2.5, 3.5]$m in steps of 0.1 m.

- Speeds are considered in the range $[50, 250]$km/h for spans in the range $[7, 15]$m. This limited speed range is adopted because S-S bridges of those spans are not usually employed for the very high speeds due to their tendency to experience strong vibration. Even if some S-S bridges below 15 m can be found in lines such as the Madrid-Sevilla, where $V = 270$ km/h, portal frames are presently regarded as a better option in such cases.

- Speeds are considered in the range $[50, 350]$km/h for spans in the range $(15, 30]$m.

- Damping ratios are selected according to EN1991-2, section 6.4.6.3.1, both for prestressed concrete and composite structures, which can be considered a conservative lower bound[**?**]:

  Steel/Composite

$$\begin{aligned}
&\zeta(\%) = 0.5 + 0.125\,(20 - L) \quad \text{for} \quad L < 20\,\text{m} \\
&\zeta(\%) = 0.5 \quad \text{for} \quad L \geq 20\,\text{m}
\end{aligned} \tag{13}$$

  Prestressed concrete

$$\begin{aligned}
&\zeta(\%) = 1.0 + 0.07\,(20 - L) \quad \text{for} \quad L < 20\,\text{m} \\
&\zeta(\%) = 1.0 \quad \text{for} \quad L \geq 20\,\text{m}
\end{aligned} \tag{14}$$

- Natural frequencies are selected in the lower limit of the frequency band in section 6.4.4 of EN1991-2: $n_{0,lower}(\text{Hz}) = \max\left\{80/L, 23.58\,L^{-0.592}\right\}$ for $L \in [4, 100]$m. This allows capturing the highest amplitude sub-resonances (at the higher wavelenghts), while the lower amplitude relevant ones are retained by considering a very low minimum speed of 50 km/h. Notice that even if the frequencies of the bridges were selected from the upper limit of the frequency band in section 6.4.4 of EN1991-2, which is some 2.0-2.5 times higher that the lower bound, the corresponding minimum speed of the results presented here would be increased in the same amount, thus leading to some 100-125 km/h, which is a reasonable lower speed in line with EN1991-2. The selection of $n_0 = n_{0,lower}$ is therefore to be regarded as a strategy to cover adequately the expected range of wavelengths, in conjunction with a minimum speed of 50 km/h.

- Given that lower bounds of linear mass and damping will be used, only cases where the maximum acceleration is above $3.5\,\text{m/s}^2$ will be retained as relevant. Δa and ΔV will not be computed in cases where the maximum acceleration is below such SLS level.

- The selection of a lower estimate for the linear mass greatly influences the representative examples that can be found where accelerations are above $3.5\,\text{m/s}^2$. Indeed, this is one of the most relevant parameters of the analysis, as it will be shown next. Therefore, estimates of the mass that are low enough to retain the majority of relevant cases will be adopted. As mentioned in the point above, due to the also low values adopted for

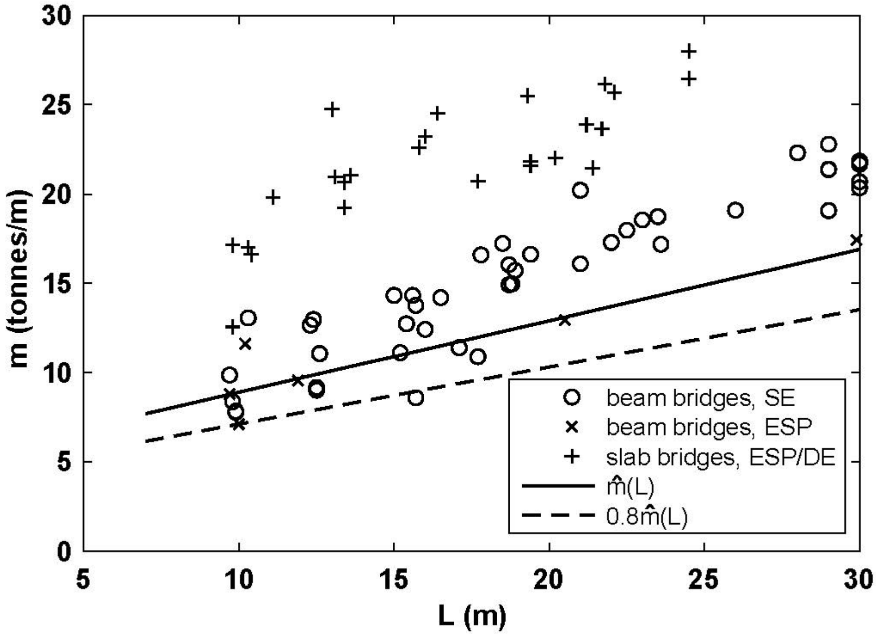

Figure 9: Linear fit of the minimum mass for single-span concrete bridges. *Slab* bridges also include filler-beam bridges.

damping, those cases found here where accelerations are below $3.5\,\mathrm{m/s^2}$ are to be deemed of little relevance. Based on a representative ensemble of single-track, concrete bridges from conventional and high-speed lines in Sweden, Spain and Germany (see Figure **??**), the following lower limit is adopted as a function of the span:

$$\hat{m}(L) = 400L + 4900 \quad \text{(kg/m) with } L \text{ in (m)} \tag{15}$$

The mass estimate in Figure **??** was obtained from design drawings for a set of real concrete bridges. All bridges considered in this study satisfy strictly the deflection limit $L/600$ under load model LM71 [**?**] for linear mass $\hat{m}(L)$, as well as for 80 % of $\hat{m}(L)$ —to be used below—. For 50 % of $\hat{m}(L)$ such deflection limit is also satisfied approximately if the frequency is chosen equal to $n_{0,lower}$ as defined before, and in a strict manner if the frequency is increased only slightly.

Under these conditions, the exceedance in acceleration Δa as defined in equation (**??**) has been computed with different levels of resolution in both span length and speed. Cases of interest where $\Delta a > 10 - 15\%$ will be pointed out in what follows. Also, the required speed increase ΔV has been calculated in a coherent manner for such cases of interest, *i.e.*, having increased the nominal HSLM-A effects by either 10% or 15% *before* computing ΔV. Particularly, those situations where $\Delta V > 20\%$ will be highlighted, which are the ones where HSLM-A (increased by 10–15%) does not cover the vibration effects of real Annex E trains.

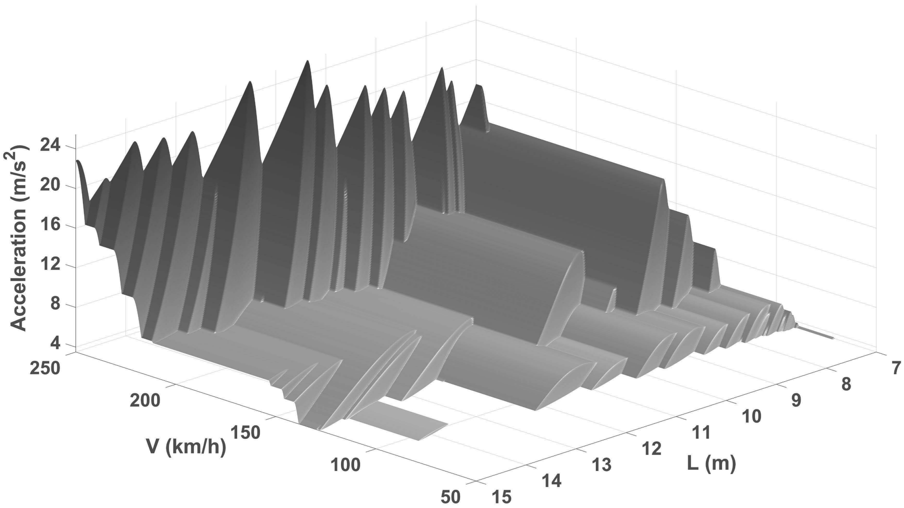

Figure 10: Cumulative maximum acceleration for HSLM-A model in prestressed concrete bridges with mass $\hat{m}(L)$: Simplified Signature approach; Load distribution not included.

It should be noticed that bridges with a very low mass as, for instance, some kinds of steel trusses with non-ballasted track, could have linear masses much lower than $\hat{m}(L)$. For this reason, such examples will deserve particular comments in the following subsections.

5.1 Concrete bridges

To begin with, (single-track) bridges with linear mass strictly equal to $\hat{m}(L)$ are discussed in this subsection. As explained before, the comparison is based on the levels of cumulative maximum response surfaces, which are plots of the kind shown in Figure **??** for the HSLM-A model. As an exception, such figure has been produced with the faster simplified signature for a finer graphical resolution.

Figures **??** and **??** compare the values of exceedance *without* and *with* load distribution for a threshold $\Delta a_{lim} = 10\%$. Since in this span range the frequency is equal to $80/L$, the lines of constant wavelength are hyperbolas in the span-vs-speed axes; this explains the curved shape of the limits of the shaded areas, given that resonance phenomena take place at particular values of wavelength. The response has been computed with the general train signature. Only those cases where $\Delta a > \Delta a_{lim}$ are shown in grey scale. The step in span length is $d_L = 0.05\,\text{m}$, while the step in speed is $d_V = 0.1\,\text{km/h}$. As it can be seen, the load distribution effect is noticeable, particularly at the lower speeds. Therefore, in order to obtain meaningful results, such distributive effect will be considered in all subsequent discussions and figures in the paper.

In some areas of Figure **??** the exceedance is above 10%, 15% or as much as 60%. Therefore, the required speed increase ΔV corresponding to Figure **??** has been calculated, and it has been found that in none of the cases it is above 20%. Therefore, the gray areas in Figure **??** are not to be deemed relevant for

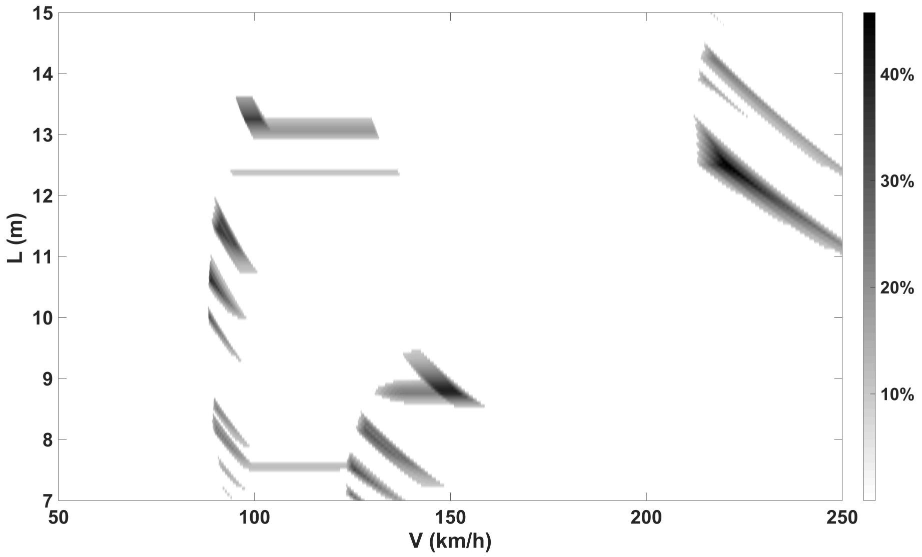

Figure 11: Exceedance Δa (only if $\geq 10\%$) for prestressed concrete bridges of mass $\hat{m}(L)$: general signature approach; Load distribution not included.

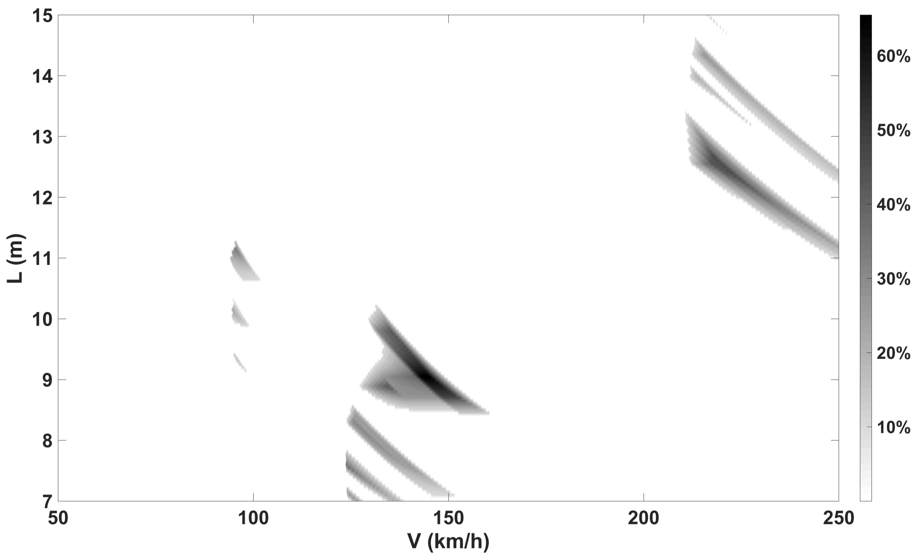

Figure 12: Exceedance Δa (only if $\geq 10\%$) for prestressed concrete bridges of mass $\hat{m}(L)$: general signature approach; Load distribution included.

dynamic assessment.

Although $\hat{m}(L)$ is a rather low value of linear mass for concrete bridges, information from design drawings may lead to overestimate the linear mass of a bridge. Therefore, bridges with even a lower value of linear mass, $0.8\,\hat{m}(L)$, have been also analysed with a view to detect if they could be relevant for the comparison of the HSLM-A *vs.* Annex E trains. Most likely such very low-mass bridges would correspond to single-track structures with slender prestressed I-girders or relatively thin-walled box sections. Under such conditions, Figure **??** reveals that there are only two significant cases occurring at speeds between some 90 and 110 km/h. Those cases corresponds to $L \simeq 12.4\,\mathrm{m}$ and $L \simeq 13\,\mathrm{m}$, and our analyses confirm that they stand out both for $\Delta a_{lim} = 10\%$ or 15%. Please recall that the low values of speed are directly related to the low frequencies selected for the bridges.

Particularly, Figure **??** shows the response of a bridge with $L = 12.4\,\mathrm{m}$ to the HSLM-A and to one real train from Annex E, having $D = 21\,\mathrm{m}$ and $b = 3.5\,\mathrm{m}$. The peak response at 175 km/h corresponds to a fifth sub-harmonic for the A4 train, a case that can be optimised according to Table **??**. The response has been computed with the general signature (the difference of the peak values is very small if time integration is used instead). Such real train is a kind of *modified A4 train* that, if added to the HSLM-A model, makes the gray area corresponding to $L = 12.4\,\mathrm{m}$ in Figure **??** turn into not relevant, even if the governing Annex E train in such gray area has $D = 20.4\,\mathrm{m}$ and produces accelerations slightly above $3.5\,\mathrm{m/s^2}$. Therefore, one possible solution to cover such case would be to incorporate the modified A4 train to the HSLM-A. In a similar manner, it can be determined that the gray area corresponding to $L \simeq 13\,\mathrm{m}$ would be covered by adding one modified A1 train ($D = 18\,\mathrm{m}$), with $b = 3.5\,\mathrm{m}$. That would imply to optimise A1 for the fourth sub-harmonic, as suggested by Table **??**.

However, adding two new trains to the HSLM-A load model with the sole purpose of covering two isolated cases would not be a convenient solution for practical applications. Instead, it is preferable that both such cases be pointed out as requiring a particularly detailed analysis, in the event that an assessment of its dynamic behaviour were required.

It is of particular interest to point out that the two relevant cases in Figure **??** stand out because the linear mass has been reduced by 20% with respect to $\hat{m}(L)$. The mass of the bridge, therefore, reveals as an important parameter for obtaining meaningful examples. This fact will be confirmed also in the following subsection.

When the previous analysis is extended for concrete bridges of $L \in (15, 30]$m and $V \in [50, 350]$km/h, the only significant case that can be found is equivalent to the one already shown in Figure **??**, but then $\Delta V < 5\%$ and such case is again not relevant.

Additionally, no further relevant cases have been found in the whole range of spans for $\hat{m}(L)$ increased by 50%, which would be a linear mass value closer to the levels expected in double-track bridges.

The results described here have been confirmed by an independent parametric study where the response has been computed by time integration of the equations of motion (which is accurate also for non-resonant response) and $d_L = 0.1\,\mathrm{m}$, $d_V = 0.5\,\mathrm{km/h}$.

In conclusion, given the hypotheses adopted for our analyses, it can be stated that the HSLM-A model covers well the dynamic response of simply supported

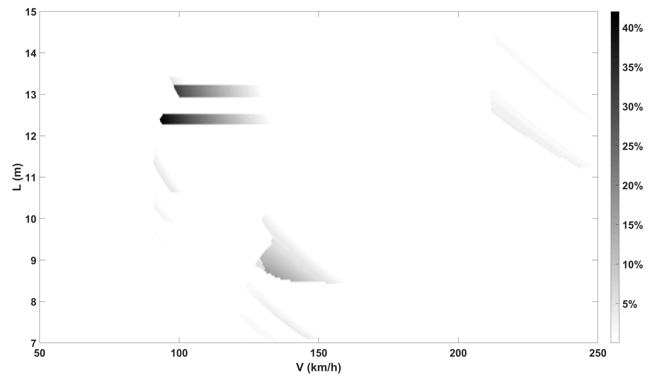

Figure 13: Speed increase ΔV required for $1.10 \cdot$ HSLM-A to cover Annex E trains. Prestressed concrete bridges of mass $0.8\,\hat{m}(L)$: general signature approach; load distribution included.

concrete bridges as regards the maximum vertical accelerations, with the exception of the few cases mentioned in this section.

5.2 Composite/Steel bridges

In order to futher analyse the validity of the preceding conclusions, some of the analyses have been repeated for bridges with damping corresponding to steel/composite structures, according to EN1991-2.

Given that these bridges are usually of mass rather low compared to concrete structures, it is unlikely that short S-S composite or steel bridges would be deemed adequate for use at speeds above 200 km/h. Nevertheless, the term *short* is necessarily imprecise in this context, given that the policies of different *Railway Administrators* may often vary among different countries. Therefore, in a view to offering some practical insight for a range of spans that can be considered more habitual for composite/steel bridges, in this paper the behaviour of such structures has been analysed for spans $L \in (15, 30]$m and speeds $V \in [50, 350]$km/h. Subsequently, further extension of the analysis to spans up to 50 m has revealed no additional relevant cases.

As it was mentioned before, the minimum values of linear mass of composite/steel bridges are often significantly lower than for concrete bridges. After the analysis of five single-span, single-track examples in the Swedish railway network, linear masses around $0.6\hat{m}(L) - 0.8\hat{m}(L)$ have been found for girder bridges and for orthotropic decks. Moreover, masses as low as 2500 kg/m have been found for truss bridges without ballast that were located in northern lines, where the operating train speeds are not high. However, the analysis of these five examples cannot of course cover all possibilities, and more comprehensive information would be needed regarding the lowest levels of mass to be expected in composite/steel structures potentially used for $V > 200$ km/h.

In order to overcome such lack of more comprehensive information, a sensitivity analysis has been performed by considering, in addition to mass equal to $\hat{m}(L)$ and $0.8\hat{m}(L)$, also a lower bound equal to $0.5\hat{m}(L)$. Since truss bridges with no ballast could present even lower values of mass, they may probably

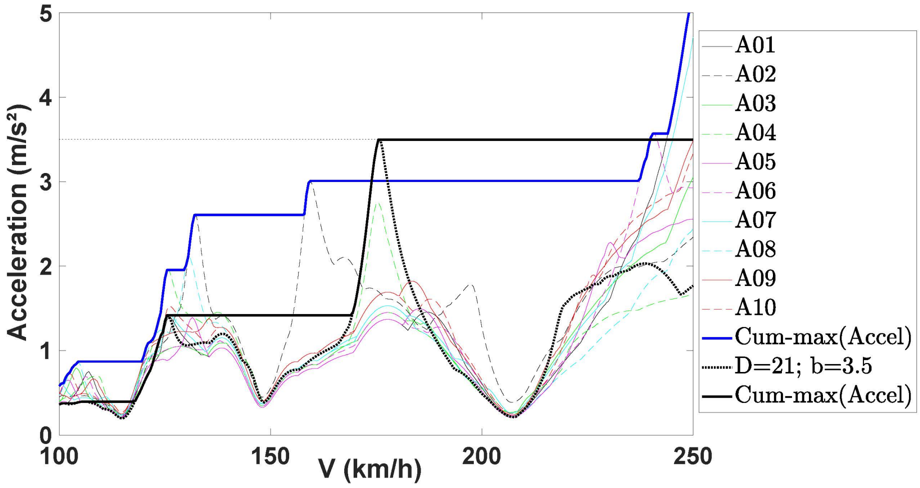

Figure 14: Maximum acceleration (general signature, one mode) at mid-span in a simply supported bridge defined by: $L = 12.4\,\mathrm{m}$, $m = 7900\,\mathrm{kg/m}$, $f = 11.6\,\mathrm{Hz}$, $\zeta = 1.53\%$.

not be covered by the results presented here and thus deserve further specific studies.

As a first conclusion, it can be stated that no relevant cases are found for bridges with mass equal to either $\hat{m}(L)$ or $0.8\hat{m}(L)$: in those situations the HSLM-A model covers the Annex E trains in the sense explained in previous sections.

Conversely, some relevant cases appear for bridges with $0.5\hat{m}(L)$, which has also been confirmed by repeating the parametric study with the time integration procedure and $d_L = 0.1\,\mathrm{m}$, $d_V = 0.5\,\mathrm{km/h}$. Figure **??** shows the most significant cases. They are relevant because in all of them the required ΔV for $1.15 \cdot$ HSLM-A to cover the Annex E trains is larger than 20%. The governing bogie wheelbase in such cases is monotonously $b = 3.5\,\mathrm{m}$.

The speeds where such cases appear are low, around 55–85km/h, which is a consequence of the frequency of the bridges being equal to $n_{0,lower}$. The associated resonant peaks take place at wavelengths around 3.5–4.5m. Nevertheless, for bridges in the upper limit of the frequency band in section 6.4.4 of EN1991-2 ($n_{0,upper}(\mathrm{Hz}) = 94.76\,L^{-0.748}$) they turn into speeds than can be above 150 km/h. Thus, could these cases be deemed relevant for a dynamic assessment according to EN1991-2, given that the prescribed initial speed[**?**] is $40\,\mathrm{m/s} = 144\,\mathrm{km/h}$?

To answer this question it should be born in mind that in any line for speed greater than 200 km/h, say $V_{\mathrm{nom}} = 210\,\mathrm{km/h}$, the design speed to be used with HSLM-A would be $V_{\mathrm{max}} = 1.2 \cdot 210 = 252\,\mathrm{km/h}$. Therefore, if the speed increase ΔV for the cases in Figure **??** is not high enough to exceed 252 km/h, HSLM-A will govern and the cases will not be relevant. Providing that the bridges stay within the frequency band in section 6.4.4 of EN1991-2 ($n_{0,lower} \leq n_0 \leq n_{0,upper}$), our analyses confirm that 252 km/h are not exceeded. If the bridge frequencies were higher (out of the band), then the cases in Figure **??** could

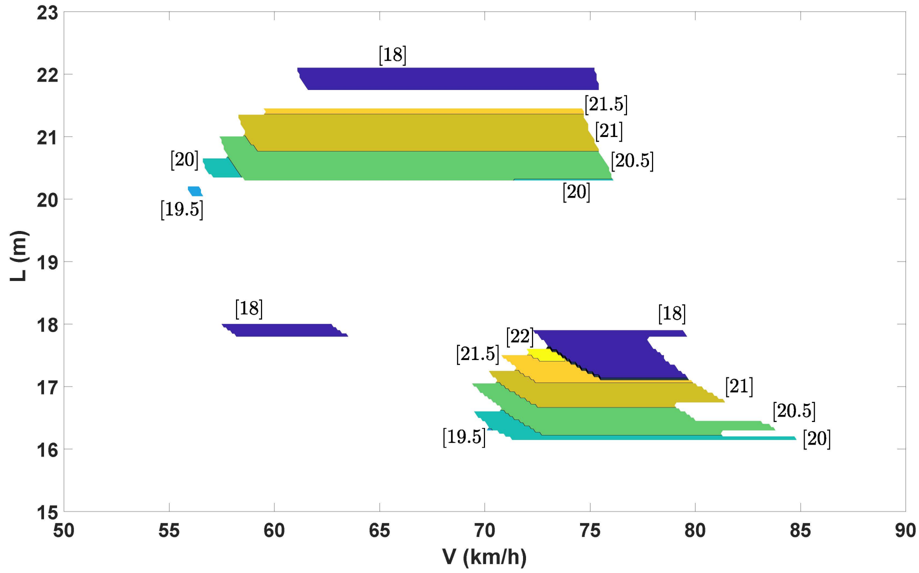

Figure 15: Coach length of Annex E governing trains in the ranges where the response is not covered by $1.15 \cdot$ HSLM-A, for steel/composite bridges of mass $0.5\hat{m}(L)$.

be determinant for dynamic assessment. Figure **??** shows the case closest to the limit: the value of ΔV highlighted between two black dots is rather large ($243\,\text{km/h} - 170\,\text{km/h} = 73\,\text{km/h} \rightarrow 43\%$), but the frequency of the bridge, being limited to the band of EN1991-2, is not high enough for the situation to be determinant in a dynamic assessment at speeds $V > 243/1.2 = 202.5\,\text{km/h}$,which is equivalent in practice to $V > 200\,\text{km/h}$.

6 Conclusions

The effects of vibrations induced by load models of articulated trains (ATs) have been analysed in this paper, with particular attention to the response of simply supported bridges. From the results of this research, the following conclusions can be extracted:

1. Of particular importance to vehicle manufacturers is that Annex E/EN1991-2 establishes that the dynamic effects of ATs with $\eta = D/d_{BA}$ ratio close to integer values may not be duly covered by model HSLM-A. Such statement conveys the idea that trains with integer η ratios can be significantly more aggressive than other trains. From a mathematical perspective, the results of this work show that this is not the case: the effects of η close to integer values are only maximal when such value is equal to the inverse of the sub-resonance order, and even in those cases the difference with other non-integer ratios is not large. The analysis carried out here encompasses the first 10 sub-harmonics of carriage resonance, within the realistic ranges of D and $b = d_{BA}$ defined in Annex E.

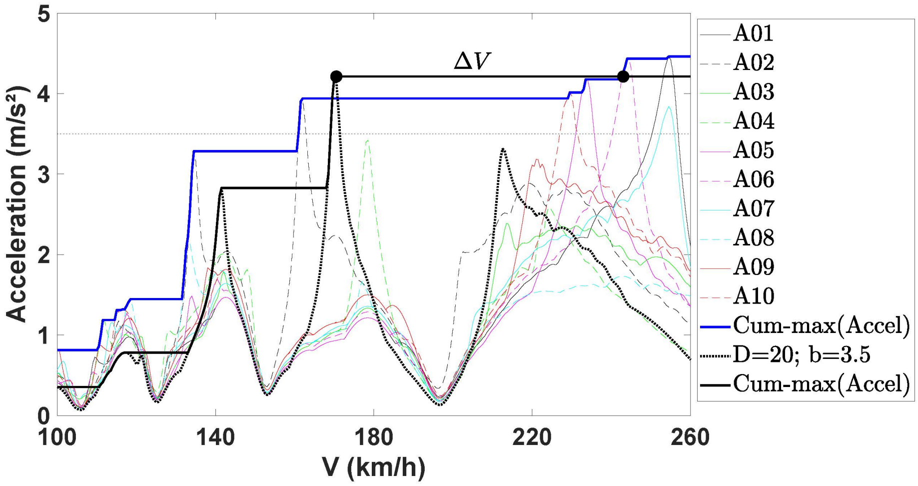

Figure 16: Maximum acceleration (general signature, one mode) at mid-span in a simply supported bridge defined by: $L = 16.2\,\text{m}$, $m = 5700\,\text{kg/m}$, $f = 11.8\,\text{Hz}$, $\zeta = 0.98\%$. Results for HSLM-A increased by 15%.

2. As a general conclusion regarding structural design, the HSLM-A model covers well the vibration (acceleration) effects of Annex E ATs for simply supported concrete bridges of spans between 7 m and 30 m, in usual ranges of speed for such bridge types. The effects in composite/steel bridges of spans between 15 m and 30 m will be also covered except for very high frequency bridges. For very low mass bridges (less than 50% of the minimum mass assumed herein for concrete bridges), the conclusions presented here could possibly not be valid and require further research.

3. A new simplified expression of the train signature has been developed for ATs. The mathematical demonstration is given in Appendix B. For wavelengths $\lambda > 4.2\,\text{m}$, the approximation to the true signature is very good both for the HSLM-A model as well as for the (articulated) trains defined in Annex E of EN1991-2. The computational cost of the new simplified signature is one order of magnitude lower than that of the general signature.

4. Based on the new train signature at resonance, the number of loads required to build up the different sub-resonances has been studied for different levels of damping. The first resonance requires a large number of loads to reach 90% or more of its maximum amplitude, which can be up to 30–40 loads for damping around 1%. The second resonance needs approximately half the number of loads, compared to the first one. The third and successive resonances need not necessarily very long trains to reach values close to their maxima, except when damping is very low.

5. The bogie wheelbase of the ten HSLM-A trains is not optimal in order to maximize all possible sub-harmonics of carriage resonance for $D \in$

[18, 27]m. Still, this lack of optimal d_{BA} values is not always significant because *previous* resonances (at lower speeds) of other HSLM-A trains cover, in many cases, the situations when one of the bogies does not have an optimal wheelbase.

6. Both the general signature and time integration have been used to analyse whether the HSLM-A model covers the effects of Annex E ATs on simply supported high-speed bridges, with tolerances of 10–15% in amplitude and 20% in speed. It has been shown that only two examples are relevant for concrete structures of spans between 7 m and 30 m (shorter spans ought to be analysed with model HSLM-B). The minimum values of linear mass, as well as the load distribution due to track and ballast, play a decisive role for finding relevant examples where accelerations are above $3.5\,\text{m/s}^2$. The two cases to be pointed out correspond to spans $L \simeq 12.4\,\text{m}$ and $L \simeq 13\,\text{m}$. In the rest of cases model HSLM-A covers the Annex E ATs as regards the vertical accelerations.

7. Because linear mass is a key factor when it comes to finding relevant cases, mass values reduced down to 50% of the ones corresponding to concrete bridges have also been analysed in conjunction with damping for composite/steel structures, in spans between 15 m and 30 m. The cases found where the HSLM-A does not cover the effects of Annex E trains correspond to resonant peaks at wavelengths around 3.5-4.5m. Such cases will not be relevant for dynamic analysis if the bridge frequencies lie within the frequency band in section 6.4.4 of EN1991-2.

7 Appendix A: Resonant response of railway bridges computed by the LIR method

The first step in order to apply the LIR method is to obtain the *free vibration* levels created by a single concentrated load of constant value F. If the bridge or structure travelled by the load is much shorter than the train, then the free vibrations arising from each load (represented by *decaying sinusoidal functions*) will accumulate with the previous ones[**?**]. This will typically be the case for actual high-speed trains, which total length is between some 200 m and 400 m (see Annex E from EN1991-2[**?**]), passing over bridges of less than typically 40 m span. Particularly, simply supported spans below 40 m have been thoroughly investigated in the last decades due to its higher propensity to undergo excessive vibration[**?**].

If the cumulative effect of successive loads is in phase, this will result in a resonant phenomenon. In such conditions it is expected that the maximum response will be obtained approximately when the last loads leave the bridge. Nevertheless, the end effects induced by the irregular distances in the load pattern of the power cars (non-repetitive distances) can sometimes modify the expected values to a certain exent[**?**].

After the load has left the bridge, the maximum acceleration in the bridge is Γ_{max}, as given by equation (**??**). Such vibration will be damped out by dissipation mechanisms that are usually expressed as a viscous effect by means of the ζ damping ratio. Then, the vibration amplitude will adopt the shape of a damped sinusoid as follows:

$$a(t) = \Gamma_{max} \mathrm{e}^{-\zeta\omega t} \sin(\omega t) \tag{16}$$

where ω is the frequency of the mode of vibration that can be either damped or undamped. For small damping, both can be considered equal for practical purposes.

Therefore, the superposition of the vibrations $a_i(t) = F_i a(t)$ created by successive loads F_i, which are separated by space intervals d_i from the first load that left the bridge is to be carried out as a summation of out-of-phase damped sinusoids. For such purpose it is central to realize that the Γ_{max} value will be a constant, common factor that will not depend on either the F_i or d_i values.

Consequently, superposition is carried out by adding the maximum free vibration created by the *last load* that leaves the bridge, plus the free vibrations created by the *preceding loads*. Resonance will occur when such addition happens to be in phase, *i.e.* when each sinusoid is an integer number of periods delayed with respect to the rest of sinusoids. Should this happen, the amplitude will grow with each load and will be only limited by damping until the last load effectively exits the structure. Conversely, if one of the loads is out of phase, then the vibration adds but just to some extent, or cancels to some extent. If damping is neglected, total cancellation will happen if one free vibration is delayed exactly half period more (or less) than an integer number of periods with respect to another vibration of the same amplitude (*i.e.* created by an identical force). This well-known[?],[?],[?],[?] mechanism of cancellation is referred in the paper as *cancellation by addition*, with a view to distinguish it from the zeroes of the influence line Γ_{max}. Such zeroes of the influence line take place at particular speeds depending on the bridge characteristics[?],[?], and usually are designated simply as *cancellations*.

It is important to notice that, since the d_i values are fixed for each particular train, resonance will occur at given speeds when the time interval between the sinusoids coincides with integer multiples of $T = 1/f = 2\pi/\omega$, being f the natural frequency in Hz. Cancellation (by addition) can be explained in much the same way, but adding or subtracting one half-period. For convenience, the so-called *wavelength* is established as a measure of the speed of the load in relation with *how fast* the structure vibrates. It represents the length travelled by the load during one period of vibration of the structure:

$$\lambda = VT \tag{17}$$

Therefore, if a train is characterized by a repetitive scheme of distances d_i (typically associated to the car length D), resonance will happen when the wavelength is equal to D or any sub-multiple: $\lambda = D/j$ where $j = 1, 2, \ldots$.

In summary, according to the LIR method, the maximum acceleration (in free vibration) due to a train of passing concentrated loads can be computed as the product of two factors: one is Γ_{max}, which depends solely on the nondimensional speed K and the bridge, while the other depends on the values F_i and d_i (*i.e.* on the pattern of loads of the train), on the wavelength and the structural damping:

$$a_{max} = \Gamma_{max}(mL, \zeta, K) \cdot G(F_i, d_i, \lambda, \zeta) \tag{18}$$

In general, equation (**??**) will not give the exact value of the maximum acceleration because this may take place when some of the loads are still on the bridge (*forced vibration*), but it has been proved that the approximation of equation (**??**) to the true maximum acceleration is very good, particularly for the resonant speeds[**?**]. The term $G(F_i, d_i, \lambda, \zeta)$ is the train signature as given by equation (**??**).

8 Appendix B: Derivation of the signature for a train of equidistant loads

Departing from equation (**??**), a train of k equidistant loads of equal modulus F, separated by a constant distance D from each other can be obtained as follows.

First, the distance of each load to the first one are expressed as

$$d_i = D(i-1) \quad \Longrightarrow \quad \delta_i = D\lambda(k-i) = k - i\Lambda \tag{19}$$

Then, the general signature in equation (**??**) is rewritten as the modulus of a complex number:

$$G = |Z| = \left| \sum_{i=1}^{k} \left(F \mathrm{e}^{-\zeta 2\pi \delta_i} \mathrm{e}^{j2\pi\delta_i} \right) \right| \qquad j = \sqrt{-1} \tag{20}$$

By substituting equation (**??**) into equation (**??**) one gets

$$Z = F\, \mathrm{e}^{2\pi(j-\zeta)k/\Lambda} \sum_{i=1}^{k} \left(\mathrm{e}^{-2\pi(j-\zeta)/\Lambda} \right)^i \tag{21}$$

The summation in equation (**??**) is a geometric progression and can be summed in a standard manner, providing that the ratio of the progression ($\mathrm{e}^{-2\pi(j-\zeta)/\Lambda}$) is not equal to one. If one examines such ratio in detail, for it being equal to one it is required that

$$\mathrm{e}^{2\pi\zeta/\Lambda} \mathrm{e}^{-j2\pi/\Lambda} = 1 \tag{22}$$

Because the second factor in equation (**??**) is a complex number, it is clear that its imaginary part must equal zero, thus

$$2\pi/\Lambda = m \cdot \pi \qquad m = 0, 1, 2, \ldots \tag{23}$$

When equation (**??**) is satisfied, then the second factor in equation (**??**) is the cosine of a multiple of π, *i.e.* $\cos(m\pi) = (-1)^m \quad m = 0, 1, 2, \ldots$. Therefore, equation (**??**) can be written as

$$\mathrm{e}^{2\pi\zeta/\Lambda}(-1)^m = 1 \qquad m = 0, 1, 2, \ldots \tag{24}$$

The factor $(-1)^m$ must be positive, *i.e.* $m = 2n, \quad n = 0, 1, 2, \ldots$ for equation (**??**) to be safistied, which leads to the resonance (or sub-resonance) case, according to equation (**??**):

$2\,\pi/\Lambda = 2n\pi \qquad n = 0, 1, 2, \ldots \quad \Longrightarrow$

$\Lambda = VT/D = 1/n \qquad n = 1, 2, \ldots$

where $n = 0$ must be excluded in real applications because VT is a finite scalar value and $D > 0$ in a train of equidistant loads. The physical interpretation of an infinitely small value of n, leading to $\Lambda \to \infty$, would be a theoretical infinite wavelength VT or an almost null distance D, such that the free vibrations from all loads on the bridge took place simultaneously (acting as a single concentrated load). This can be easily confirmed by extending the horizontal axis in Figure **??** and observing that $G_E \to k$ for high values of Λ (particularly when $\Lambda > k$).

Because damping ratio ζ must be zero for equation (**??**) to hold, then it can be stated that the geometric progression can always be summed in a standard manner except for the *undamped resonance case.* This particular case will be treated afterwards.

The sum of the geometric progression in equation (**??**) yields the complex signature Z as follows:

$$Z = F\, \mathrm{e}^{2\pi(j-\zeta)k/\Lambda} \mathrm{e}^{-2\pi(j-\zeta)/\Lambda} \left(\mathrm{e}^{-2\pi(j-\zeta)k/\Lambda} - 1\right) \mathrm{e}^{-2\pi(j-\zeta)/\Lambda} - 1 \tag{25}$$

By multiplying the numerator and denominator by $\mathrm{e}^{j2\pi/\Lambda}\mathrm{e}^{\zeta 2\pi/\Lambda} - 1$ one gets, after some algebra, an expression where the denominator is real:

$$\begin{aligned} Z &= F\, A - BC \\ A &= \mathrm{e}^{\zeta 2\alpha} - \mathrm{e}^{-j\alpha}\, \mathrm{e}^{\zeta\alpha} \\ B &= \mathrm{e}^{jk\alpha} \mathrm{e}^{\zeta(2-k)\alpha} - \mathrm{e}^{-j(1-k)\alpha} \mathrm{e}^{\zeta(1-k)\alpha} \\ C &= \mathrm{e}^{\zeta 2\alpha} - 2\, \mathrm{e}^{\zeta\alpha} \cos(\alpha) + 1 \\ \alpha &= 2\pi/\Lambda \end{aligned} \tag{26}$$

Equation (**??**) can be used to obtain the real and imaginary parts of Z as follows:

$$\begin{aligned} \mathtt{Re}(Z) &= F\, \Big(\mathrm{e}^{\zeta 2\alpha} - \mathrm{e}^{\zeta\alpha}\cos(\alpha) - \mathrm{e}^{\zeta(2-k)\alpha}\cos(k\alpha) \\ &\quad + \mathrm{e}^{\zeta(1-k)\alpha}\cos((1-k)\alpha)\Big)/C \\ \mathtt{Im}(Z) &= F\, \Big(\mathrm{e}^{\zeta\alpha}\sin(\alpha) - \mathrm{e}^{\zeta(2-k)\alpha}\sin(k\alpha) \\ &\quad - \mathrm{e}^{\zeta(1-k)\alpha}\sin((1-k)\alpha)\Big)/C \end{aligned} \tag{27}$$

From equation (**??**) the signature can be evaluated as the modulus of Z. After some simplifications, and by including $C = f_1(\sigma, \Lambda)$ from equation (**??**) into the square root that will yield the modulus of Z, one gets precisely equation (**??**) when force F is set equal to unity.

As regards the undamped resonance case, in such condition it will be verified that $2\pi\delta_i = 2\pi(k - i)/\Lambda$, where $\Lambda = 1, 1/2, 1/3, \ldots$, which implies that $2\pi\delta_i$ will be either zero (if $i = k$) or a multiple of 2π (otherwise). Therefore, the sine functions vanish in equation (**??**). Besides, in equation (**??**) $\theta_i = 1$ and the cosine functions will be also equal to one. Then, for unit loads F, the signature is simply equal to the number of equidistant loads k.

This research was partially developed during a stay performed by Pedro Museros at the *KTH Royal Institute of Technology*, within the Division of Structural Engineering and Bridges (Stockholm, Sweden). The financial support of the *Generalitat Valenciana*, through the program BEST2019 for research stays (*Subvenciones para estancias de personal investigador doctor en centros de investigación radicados fuera de la Comunitat Valenciana*), as well as the permission obtained from the *Universitat Politècnica de València* to carry out such stay, are gratefully acknowledged.

9 Declaration of Conflicting Interests

The Authors declare that there is no conflict of interest.

References

[Ford (1992)] Ford R.A.J. *Track and ground vibrations from trains running on conventional ballasted track. P I Mech Eng-J Rai*, 1992; 206(2):117-126.

[Auersch (2006)] Auersch L. *Ground vibration due to railway traffic—The calculation of the effects of moving static loads and their experimental verification. J Sound Vib*, 2006; 293:599-610.

[Krylov and Ferguson (1994)] Krylov V.V. and Ferguson C.C. *Calculation of low-frequency ground vibrations from railway trains. Appl Acoust*, 1994; 42:199-213.

[Shin et al (2010)] Shin J.R., An Y.K., Sohn H. and Yun C.B. *Vibration reduction of high-speed railway bridges by adding size-adjusted vehicles. Eng Struct*, 2010; 32(9):2839-2849.

[Milne et al. (2017)] Milne D.R.M., Le Pen L.M., Thompson D.J. and Powrie W. *Properties of train load frequencies and their applications. J Sound Vib*, 2017; 397:123-140.

[Vestroni and Vidoli (2007)] Vestroni F. and Vidoli S. *Closed-form solutions for the structural response to train loads. J Sound Vib*, 2007; 303:691-706.

[Matsuoka et al. (2019)] Matsuoka K, Collina A, Somaschini C. and Sogabe M. *Influence of local deck vibrations on the evaluation of the maximum acceleration of a steel-concrete composite bridge for a high-speed railway. Eng Struct*, 2019; 200:109736.

[ERRI RP6(1999)] European Rail Research Institute (D-214 Committee, ERRI D-214). *Rail bridges for speeds > 200 km/h. Calculations for bridges with simply supported beams during the passage of a train (RP6).* 1999.

[Eurocode 1(2003)] European Committee for Standardisation (CEN).EN1991-2.*Eurocode 1: Actions on structures. Part 2: General Actions – Traffic Loads on Bridges.* September 2003.

[Savin (2001)] Savin E. *Dynamic amplification factor and response spectrum for the evaluation of vibrations of beams under successive moving loads. J Sound Vib*, 2001; 248(2):267-288.

[Bishop and Djuric (1996)] Bishop W.B. and Djuric P.M. *Model order selection of damped sinusoids in noise by predictive densities. IEEE T Signal Proces*, 1996; 44(3):611-619.

[Domenech et al. (2014)] Doménech A., Museros P., Martínez-Rodrigo M.D. *Influence of the vehicle model on the prediction of the maximum bending response of simply-supported bridges under high-speed railway traffic. Eng Struct*, 2014; 72:123-139.

[Yau et al. (2019)] Yau J.D., Martínez-Rodrigo M.D. and Doménech A. *An equivalent additional damping approach to assess vehicle-bridge interaction for train-induced vibration of short-span railway bridge. Eng Struct*, 2019; 188:469-479.

[ERRI RP9(1999)] European Rail Research Institute (D-214 Committee, ERRI D-214). *Rail bridges for speeds > 200 km/h. Final report (RP9).*, 1999.

[Eurocode 0 A1(2005)] European Committee for Standardisation (CEN).EN1990:2002/A1:2005.*Eurocode: Basis of structural design – Annex A2.* December 2005.

[Yang et al. (1997)] Yang Y.B., Yau J.D., Hsu L.C. *Vibrations of simple beams due to trains moving at high speeds. Eng Struct*, 1997; 19(11):936-944.

[Museros et al. (2013)] Museros P., Moliner E. and Martínez-Rodrigo L. *Free vibrations of simply-supported beam bridges under moving loads: Maximum resonance, cancellation and resonant vertical acceleration. J Sound Vib*, 2013; 332:326-346.

[Moliner et al. (2017)] Moliner E., Martínez-Rodrigo M.D., Museros P. *Dynamic performance of existing double track railway bridges at resonance with the increase of the operational line speed. Eng Struct*, 2017; 132:98-109.

[Zangeneh et al. (2019)] Zangeneh A., Battini J.M., Pacoste C. and Karoumi R. *Fundamental modal properties of simply supported railway bridges considering soil-structure interaction effects. Soil Dyn Earthq Eng*, 2019; 121:212-218.

[Museros and Moliner (2017)] Museros P. and Moliner E. *Comments on Vibration of simply supported beams under a single moving load: A detailed study of cancellation phenomenon by C.P. Sudheesh Kumar, C. Sujatha, K. Shankar [Int.J.Mech.Sci.99(2015) 4047,doi:10.1016/j.ijmecsci.2015.05.001]. Int J Mech Sci*, 2017; 128-129:709-713.

[Museros and Alarcon (2005)] Museros P. and Alarcón E. *Influence of the second bending mode on the response of high-speed bridges at resonance. J Struct Eng*, 2005; 131(3):405-415.

[ERRI$_D$214$_2RP$1(2002)] European Rail Research Institute (D-214.2 Committee, ERRI D-214.2). *Use of universal trains for the dynamic design of railway bridges. Summary of results of D-214.2.* 2002.

[UIC$_7$76$_2R$(2003)] Union Internationale des Chemins de Fer. *UIC Code 776-2R: Design requirements for rail bridges based on interaction phenomena between train, track, bridge and in particular, speed.* 2003.

[Jin et al(2005)] Jin Z., Huang B., Ren J. and Pei S. *Reduction of vehicle-induced vibration of railway bridges due to distribution of axle loads through track. Shock Vib*, 2018; Article ID 2431980, 14 pages.

[Axelsson et al(2005)] Axelson E., Syk A. Ülker-Kaustell M., Battini J.M. *Effect of Axle Load Spreading and Support Stiffness on the Dynamic Response of Short Span Railway Bridges. Struct Eng Int*, 2018; 24(4):457-465.

[Xia et al. (2014)] Xia H., Li H.L., Guo W.W. and De Roeck G. *Vibration resonance and cancellation of simply supported bridges under moving train loads. J Eng Mech*, 2014; 140(5):04014015